Rolling Contact Crack Growth in a PMMA Disc

S. I. AL-SABTI, T. A. STOLARSKI

Department of Mechanical Engineering, Brunel University, Uxbridge, Middlesex UB8, 3PH, United Kingdom

Received 13 March 2000; accepted 15 March 2000

ABSTRACT: A two-disc machine was used to study crack propagation rate in polymethylmethacrylate (PMMA) subjected to cyclic loading created by a rolling contact. An initial crack of known length was created in PMMA disc, and its growth under known load conditions continuously monitored. It appears that after initial rapid crack growth there is a period of noticeable reduction in the crack growth rate. A rate equation based on the Paris approach is derived and its coefficients found to be $m_p = 0.705$ and $C_p = 2.93 \times 10^{-4}$. © 2000 John Wiley & Sons, Inc. J Appl Polym Sci 78: 2311–2317, 2000

Key words: PMMA; two-disk machine; crack propagation

INTRODUCTION

Bulk fatigue of polymers has been the subject of studies for the last 40 years. [1–3] As a result of that, it is now commonly accepted that polymer fatigue can occur either by thermal softening and melting due to a massive hysteric heating or by fatigue crack initiation and propagation leading to fracture.[4] The latter will occur during fatigue testing at low applied stresses or low frequencies as a result of craze breakdown. This is particularly true for brittle polymers like polymethylmethacrylate (PMMA) Unlike cracks, crazes are characterized by an inner structure of heavily plastically deformed polymeric material and by relatively sharp boundaries to the undeformed surrounding. The initiation of crazes and cracks can often be correlated with heterogeneities at the surface of the sample such as scratches and notches or with the cyclic straining process itself. The crazes will grow in length and thickness. Failure occurs due to crack initiation and propagation inside the crazes, at the boundaries of the craze and in places where the crazes may rupture spontaneously under the influence of local field of increased stress. Cracks inside the crazes propagate by excessive overstressing and rupture of the fibrils. These cracks will propagate quickly, almost without absorbing energy.

Rolling contact fatigue is an important issue affecting the performance of gears, rolling-element bearings, rolls in the steel making process, railway wheels and rails, and a number of other important machine elements. Numerous investigations have, therefore, been carried out by various researchers since the pioneering study by Way.[5] These studies have mainly concerned metallic rolling contacts. There is evidence that both wear and fracture under rolling contact can involve the growth of cracks below the periphery under the action of the cyclic contact stresses. [6–10] These are either preexisting crack-like defects or cracks nucleated by the cyclic plastic deformation of the rim.[9,11] The lives of rolling components are shortened when such cracks grow and become large enough to cause the fragmentation of the peripheral surface. In contrast, surface fatigue of polymers resulting from rolling contact conditions has received much less attention. It has been established, however, that some thermoplastic polymers, when tested under rolling contact conditions, posses quite satisfactory surface fatigue strength,[12] while certain thermosetting polymers

Correspondence to: T. A. Stolarski (mesttas@brunelac.uk).

Journal of Applied Polymer Science, Vol. 78, 2311–2317 (2000)

fail in a typical brittle manner.[13] Nevertheless, the understanding of the mechanisms involved in the surface fatigue process is far from being satisfactory, and is in need of further advancement.

This article presents and discusses the results of experiments with a PMMA disc in rolling contact with a steel disc. The objective was to measure the crack growth rate that is required to estimate the lives of components subjected to rolling contact. This approach is well established, and has been applied by Fleming and Suh[14] and Rosenfield[15] to the process of wear of metal rolling components, and by Keer and Bryant[16] to rolling contact fatigue. However, relatively little progress has been made toward defining relations among the contact pressure, flow geometry, and configuration. This is partly because of the difficulty of producing flawed metal test pieces that can be subjected to rolling contact and subsequent crack growth rate measurements. PMMA, as well as having high light transmissivity, nearly obeys Hooke's law under compression; large areas of contact can be achieved at moderate loads owing to its low stiffness, thereby reducing the possibility of creep while at the same time bringing crack depths up to a macroscopic level. An initial through-thickness edge crack, extending radially from the peripheral surface of the PMMA disc and of known length, was introduced into the disc and its growth monitored under carefully controlled load conditions. This crack configuration is quite difference from that used by Uzel et.al.[17]

TEST CONTACT CONFIGURATION AND CRACK LOADING CONDITIONS

Apparatus and Test Procedure

Results presented and discussed in this article were obtained in a test apparatus based on a two-disc contact configuration. The schematic representation of the apparatus in shown in Figure 1. The driving steel disc had diameter of 150 mm and thickness of 10 mm. After machining, the circumference of the disc was ground to 0.16 μm R_a. The driven disc was the test disc made of PMMA commercially available. Its diameter was 50 mm and thickness 4 mm. A normal load of 200 N applied to the contact in the form of a dead weight produced a peak contact pressure of 88 MPa (based on Hertzian stress analysis), and was kept constant throughout a given test. This load was well below that necessary to cause yielding.

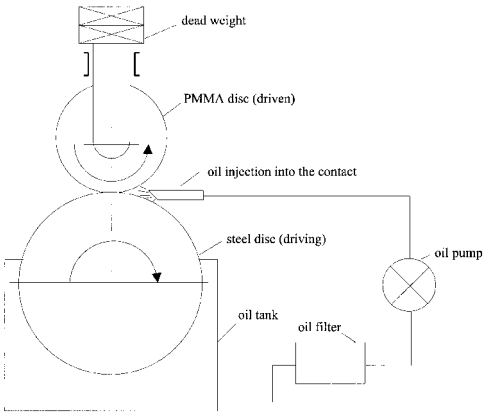

Figure 1 Schematic representation of the apparatus used to measure the rate of crack propagation under rolling contact conditions.

Discs with different lengths of installed cracks were tested. The PMMA disc was driven by the steel disc which, in turn, was powered by an electric motor coupled with a variable speed gear box. Experiments presented here were carried out at the rotational speed of a PMMA disc of 565 rpm, which corresponds to a linear speed of 1.48 ms^{-1}.

The contact between discs was lubricated by a base mineral oil containing no additives. The reason for lubricating the contact was dictated by the need to prevent premature wear damage of the PMMA disc peripheral surface before any measurable crack growth took place. Also, the unformulated lubricant was used because it did not chemically attack PMMA. It was fed into the contact region by an oil pump at a rate of 6 mL/min. Every test was interrupted at regular intervals for crack length measurements and the inspection of the contact path for signs of surface damage. When microscope examination revealed damage on the periphery of the PMMA disc, the test was terminated and the total time of running recorded. Precision crack length measurements were carried out with the help of Vidicom 300—a fully automatic, three-axis measuring instrument with a video camera utilizing a full gray-scale processing technique. Every test was repeated twice. However, if the results of these tests were different by more than 20%, a third test was conducted.

PMMA Disc Preparation

Commercial-grade PMMA, supplied by ICI in a form of a 4 mm-thick cast sheet, was used. Discs with diameter 50.3 mm were cut out. Then a

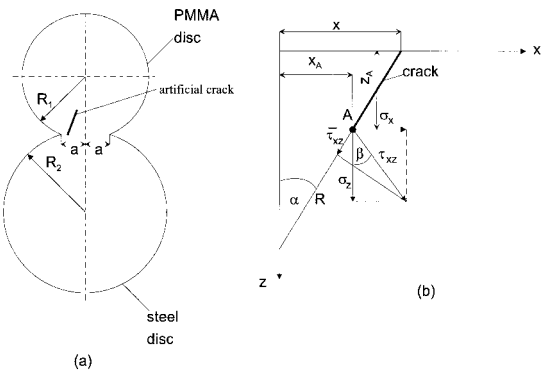

Figure 2 Geometry of contact configuration. (a) two discs in line contact, (b) coordinates of an artificially produced crack in PMMA disc.

notch was artificially created on the periphery by dropping a weight with known mass down a tube onto a chisel with a sharp tip. As a result of that, a sharply ended through-thickness notch was created with a length varying between 1.3 to 1.5 mm. The disc was then finally machined to 50-mm diameter, and unwanted cracks and imperfections created during impact removed. To avoid edge damage effects, both discs were chamfered. The final stage in the process of specimen preparation was polishing and annealing the disc to remove any residual stress that might be introduced during machining. A typical finish of the peripheral surface of the disc was 0.16 μm R_a.

Contact Geometry and Crack Loading

Figure 2 shows, schematically, all important parameters characterising contact geometry and artificial crack location. The configuration used is a line contact with a contact stress distribution as predicted by the Hertz theory. As the PMMA disc rotates under the load, the crack present in it approaches the contact zone of width, 2a, [Fig. 2(a)], passes through it, and leaves it. During that cycle, repeated every full revolution of the disc, the crack is loaded and unloaded. The load acting on the crack, positioned radially within the disc, arises from the normal contact stress, p, when the two discs are in pure rolling. Although there is a tangential stress due to microslip, it can be safely neglected here as being small due to a lubricant presence within the contact region. Also, the possibility of crack growth due to lubricant hydraulic pressure caused by ingress of oil into the crack as suggested by Way[5] has to be rejected, as the through-thickness crack was used in this study. The main requirement in the oil hydraulic pressure crack extension mechanism is the entrapment and effective sealing of the lubricant within the crack cavity—a feature clearly absent in the configuration studied. Although the stress field is compressive where the artificial crack is located, there is also a shear stress component giving rise to mode II crack loading. The principal stresses σ_x and σ_y at the location of point A (Fig. 2) are given by:[18]

$$\sigma_x = -p_{\max}\left[\left(1+\frac{2z^2}{a^2}\right)\left(1+\frac{z^2}{a^2}\right)^{-1/2} - 2\,\frac{z}{a}\right] \quad (1)$$

$$\sigma_z = -p_{\max}\left(1+\frac{z^2}{a^2}\right)^{-1/2} \quad (2)$$

The magnitude of principal shear stress, t_{xz}, is then given by,

$$\tau_{xz} = p_{\max}\left[\frac{z}{a} - \frac{z^2}{a^2}\left(1+\frac{z^2}{a^2}\right)^{-1/2}\right] \quad (3)$$

where z denotes the depth beneath the surface at which an element of material is located.

The parameters involved in the above equations are given by the Hertz theory for elastic line contact. Thus, the width of the contact, a is given by

$$a = \sqrt{\frac{4PR}{\pi E^*}} \quad (4)$$

where P is the load per unit contact length,

$$R = \left(\frac{1}{R_1}+\frac{1}{R_2}\right)^{-1}$$

is the equivalent radius of curvature of contacting discs,

$$E^* = \left(\frac{1-v_1^2}{E_1}+\frac{1-v_2^2}{E_2}\right)^{-1}$$

is the equivalent Young's modulus for materials of both discs.

The maximum contact stress is given by,

$$p_{\max} = \frac{2P}{\pi a} = \left(\frac{PE^*}{\pi R}\right)^{1/2} \quad (5)$$

The contact stress at any point within the contact zone is given by,

$$p_x = \frac{2P}{\pi a}\left(1 - \frac{x^2}{a^2}\right)^{1/2} \tag{6}$$

where $-a \le x \le a$.

From the contact geometry shown in Figure 2,

$$\sin\,\alpha = \frac{x}{R_1} \tag{7}$$

therefore,

$$\alpha = \arcsin\left(\frac{x}{R_1}\right) \tag{8}$$

The component of principal shear stress giving rise to mode II crack loading is given by the expression,

$$\tau'_{xz} = \tau_{xz}\cos(\alpha + \beta) \tag{9}$$

where

$$\beta = \frac{1}{2}\arcsin\left(\left(\frac{\sigma_x - \sigma_z}{2}\right)\frac{1}{\tau_{xz}}\right). \tag{10}$$

Coordinates of the crack tip (in Fig. 2 denoted by A) can be expressed in terms of crack length, a_c, and α, which together define the position of the crack mouth within the loaded contact zone.

$$x_A = x - a_c\sin\,\alpha \tag{11}$$

$$z_A = a_c\cos\,\alpha \tag{12}$$

Assuming that x is changing between 0 and a (i.e., half-width of the contact zone is considered only), it is possible to find out at what value of x the maximum τ'_{xz} occurs. Figure 3 illustrates the change of shear stress at the crack tip, τ'_{xz}, with the position of the crack mouth defined by x. The calculations were carried out with a contact load of 200 N and crack length, a_c = 0.987 mm. It can be seen that the maximum τ'_{xz} occurs at $x = a$, that is, when the crack enters the contact zone.

The stress intensity factor, K_{II} , for a mode II crack loading is given by,

$$K_{\mathrm{II}} = \tau'_{xz}\sqrt{\pi a_c} \tag{13}$$

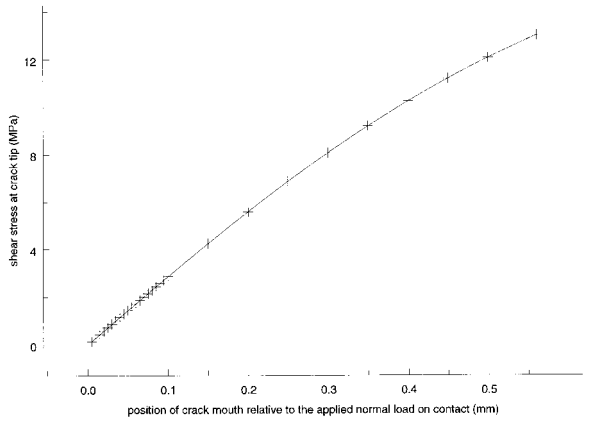

Figure 3 Shear stress at the crack tip as a function of crack mouth position relative to the normal load on the contact. Load on contact: 200 N; crack length: 0.987 mm; crack orientation: radial.

Taking into account equations introduced earlier, the final form of the equation for stress intensity factor at the crack tip is,

$$K_{\mathrm{II}} = \tau_{xz}\cos\left[\arcsin\left(\frac{a}{R_1}\right) + \frac{1}{2}\arcsin\left(\frac{\sigma_x - \sigma_z}{2}\frac{1}{\tau_{xz}}\right)\right] \tag{14}$$

where

$$\tau_{xz} = p_{\max}\left[\frac{z_A}{x_A} - \frac{z_A^2}{x_A^2}\left(1 + \frac{z_A^2}{x_A^2}\right)^{-1/2}\right] \tag{15}$$

$$\sigma_x = -p_{\max}\left[\left(1 + \frac{2z_A^2}{x_A^2}\right)\left(1 + \frac{z_A^2}{x_A^2}\right)^{-1/2} - 2\frac{z_A}{x_A}\right] \tag{16}$$

$$\sigma_z = -p_{\max}\left(1 + \frac{z_A^2}{x_A^2}\right)^{-1/2} \tag{17}$$

The following data characterize mechanical properties of contacting materials and test conditions under which results presented here were obtained. (a) Load on contact P = 200 N (this corresponds to a load per unit contact length of 50,000 N/m as the thickness of PMMA disc was 4 mm); (b) radius of PMMA disc, R_1 = 25 mm; c) radius of steel disc, R_2 = 75 mm; (d) Young's modulus (PMMA), E_1 = 3.3 GPa; (e) Poisson's ratio (PMMA), ν_1 = 0.38; (f) Young's modulus (steel), E_2 = 210 GPa; (g) Poisson's ratio (steel), ν_2 = 0.3;

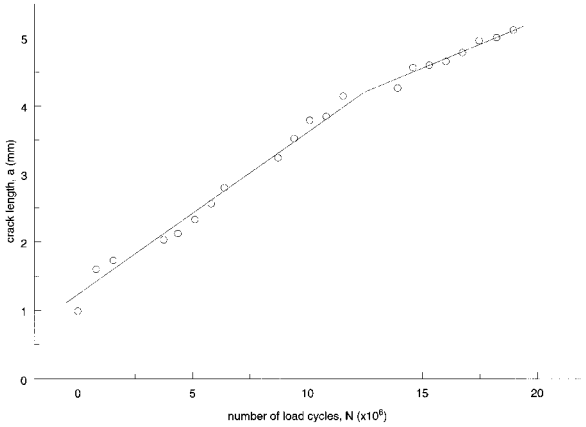

Figure 4 Crack growth as a function of the number of load cycles. Load on the contact: 200 *N*.

(h) width of the contact zone, $a = 0.562$ mm; (i) maximum contact pressure, $p_{max} = 56.8$ MPa.

RESULTS AND DISCUSSION

Crack Growth

The crack growth was monitored throughout the test by measuring the length of the crack at regular intervals of the load cycle. The results are plotted to obtain the crack growth curve as in Figure 4. The important feature of the curve shown in Figure 4 is that the growth of the crack is not a strong function of the number of load cycles applied—a usual case with ferrous materials subjected to tensile loading (mode I crack loading). Two distinct regions in the crack growth could be distinguished. The first one extends from 0 to around 13×10^6 load cycles, and the other one from 14×10^6 to 19×10^6 load cycles, which is the maximum number attained during testing. The average growth rate is 0.24 nm/cycle in the first region. The growth rate of 0.13 nm/cycle is characteristic for the second region. These growth rates are appreciable lower than that reported by Uzel et al.[17] There could be two reasons for that. First, the load on the contact in the case reported here was almost two times lower than that used by them. Second, the crack configuration used in this study was also significantly different from the configuration studied by them. The relationship between crack growth and the number of load cycles *N* is approximately linear in both regions. The self-arrest manifested by a significant reduction in the crack growth rate was probably caused by the crack growing out of the stress zone created by the rolling contact. The intensity of the compressive stress field inside the PMMA disc decreases with the distance *z* from the contact interface. Thus, as the crack grew, the load at its tip steadily decreased, which resulted in a slowdown in crack growth.

Rate Equation

The objective of any crack growth measurements is to obtain the growth rate dependence upon ΔK, which requires determination of the stress intensity range. The average crack size at Δa_{c1} is a_{c1}. The stress range is $\Delta\tau'_{xz}$, so that $\Delta K_{II} = \Delta\tau'\sqrt{\pi a_{c1}}$. Apparently, a value of $\Delta K = \Delta K_{II}$, produced crack growth at a rate of $(\Delta a_c/\Delta N_1)$. This result is plotted as a data point in a diagram with $da_c/dN(=\Delta a_c/\Delta N)$ and ΔK_{II} along the axes. The above procedure is repeated for a number of points along the crack growth curve and the curve in Figure 5 provides the growth rate for any given ΔK_{II}. It is seen that the rate is a rising function of ΔK, so, in general terms, the mathematical form of the growth rate curve is:[19]

$$\frac{da_c}{dN} = f(\Delta K) \tag{18}$$

It is an acceptable approximation to assume that the data shown in Figure 5 fall on a straight line in a logarithmic plot. The equation for a straight line is $y = mx + b$. In the present case, $y = \log(da_c/dN)$ and $x = \log(\Delta K_{II})$, so that:

$$\log\left(\frac{da_c}{dN}\right) = m_p \log(\Delta K_{II}) + \log(C_p) \tag{19}$$

Taking the antilog provides:

$$\frac{da_c}{dN} = C_p(\Delta K_{II})^{m_p} \tag{20}$$

This expression is generally known as the Paris equation. The parameters C_p and m_p can be determined easily. For example, using coordinates of two points located on the line in Figure 5, yields,

$$\log(6 \times 10^{-2}) = m_p \log(1.9 \times 10^3) + \log C_p \tag{21}$$

$$\log(7 \times 10^{-1}) = m_p \log(6.2 \times 10^4) + \log C_p \tag{22}$$

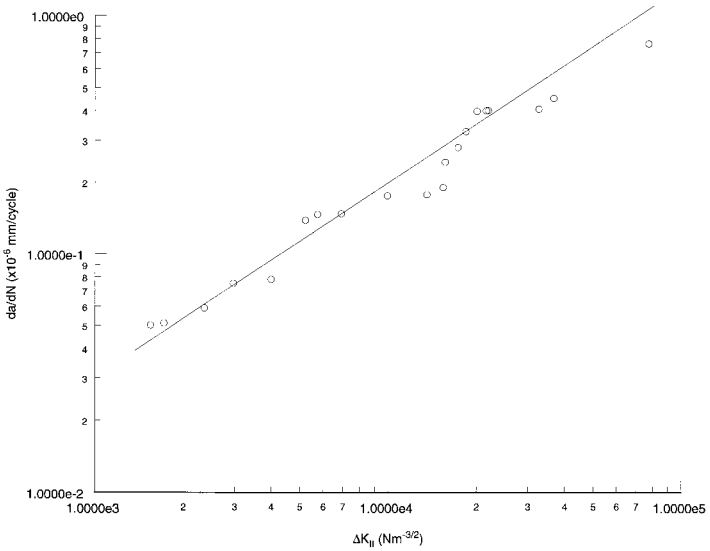

Figure 5 Crack growth rate as a function of stress intensity at the crack tip.

Taking the logarithms provides,

$$-1.22 = 3.28m_p + \log C_p \tag{23}$$

$$-0.155 = 4.79m_p + \log C_p \tag{24}$$

Subtracting sides of the above equations gives,

$$-1.065 = -1.51m_p \tag{25}$$

so

$$m_p = 0.705 \tag{26}$$

Substituting $m_p = 0.705$ in one of the equations leads to $C_p = 2.93 \times 10^{-4}$. The rate equation becomes,

$$\frac{da_c}{dN} = 2.93 \times 10^{-4}(\Delta K_{\mathrm{II}})^{0.705} \tag{27}$$

for the material investigated under the conditions described earlier.

DISCUSSION

For most materials tested in a conventional way the value of m_p is between 3 and 5. The current value of $m_p = 0.705$ is clearly different, and can be explained by the conditions of crack loading. It is apparent from Figure 4 that the crack growth rate decreases with the number of load cycles—a feature that is very much different from the crack growth vs. number of load cycles relationship observed for conventional crack loading. The value of C_p is known to be strongly material dependent, and there is no benchmark value for it. Therefore, $C_p = 2.93 \times 10^{-4}$ found for the PMMA disc in rolling contact must be accepted as representing the system investigated. It must be remembered that the Paris equation is one of many equations used to describe in best possible way the test data. But none of these, nor the equations used here, have any physical significance; they all are merely curve fitting equations. If they do fit the data properly, there is no objection against their use. The test data presented in this article are well represented by eq. (27).

CONCLUSIONS

The main objective of the study, with the results presented here, was to determine the crack growth rate in a PMMA disc subjected to cyclic mode II loading resulting from the rolling contact configuration. It was found that under the test conditions employed, the crack growth with the number of load cycles is not uniform. At the beginning of the process, the crack growth rate is quite strong, but as the crack grows longer, the rate of the growth decreases. It is believed that the stress distribution created by the rolling con-

tact can be used to explain the decrease in the crack growth rate. The rate equation based on the Paris approach was derived for the system studied. The rate equation coefficients were found to be: $m_p = 0.705$ and $C_p = 2.93 \times 10^{-4}$.

REFERENCES

1. Andrews, E. W. In Fatigue in Polymers, Testing of Polymers; Brown, W., Ed.; Wiley: New York, 1969, vol. 4.
2. Manson, J. A.; Hertzberg, R. W. Crit Rev Macromol Sci 1973, 141, 341.
3. Hertzberg, R. W. Deformation and Fracture Mechanics of Engineering Materials; Wiley: New York, 1976.
4. Stolarski, T. A. In Advances in Composite Tribology; Fridrich, K., Ed.; Elsevier Science: New York, 1993, p. 629, vol. 8.
5. Way, S. ASME J Lubricat Technol 1935, 2, A49.
6. Syniuta, W. D.; Corrow, C. J. Wear, 1970, 15, 187.
7. Martin, G. C.; Hay, W. W. ASME Paper 72-WA/RT-8, 1972.
8. Sugino, K.; Miyamoto, K.; Nagumo, M. Trans Iron Steel Inst Jpn, 1971, 11, 9.
9. Suh, N. P. Wear 1977, 44, 1.
10. Kunikake, T.; Nishimura, S.; Tagashira, H. Trans Iron Steel Inst Jpn 1970, 10, 476.
11. Fegredo, D. M.; Pritchard, C. Wear 1978, 49, 67.
12. Lawrence, C. C.; Stolarski, T. A. Wear 1989, 132, 183.
13. Stolarski, T. A.; Hosseini, S. M.; Tobe, S. Wear 1998, 214, 271.
14. Fleming, J. R.; Suh, N. P. Wear 1977, 44, 39.
15. Rosenfield, A. R. Wear 1980, 61, 125.
16. Keer, L. M.; Bryant, M. D.; Haritos, G. K. ASME J Lubricat Technol 1982, 104, 347.
17. Uzel, A. R.; Gentle, C. R.; Hills, D. A. Wear 1985, 106, 341.
18. Johnson, K. L. Contact Mechanics; Cambridge University Press: New York, 1985.
19. Broek, D. The Practical Use of Fracture Mechanics; Kluwer Academic Publishers; The Netherlands, 1985.